Published in final edited form as:
Langmuir. 2013 February 26; 29(8): 2700–2707. doi:10.1021/la304129y.

Predicting Isoelectric Points of Non-functional Mitochondria from Monte Carlo Simulations of Surface Compositions

Gregory G. Wolken, **Benjamin J. Fossen**, **Ayoung Noh**, and **Edgar A. Arriaga***
Department of Chemistry, University of Minnesota, Minneapolis, Minnesota 55455, United States

Abstract

Mitochondria are heterogeneous organelles involved in energy production, metabolism, and cellular signaling that oftentimes are isolated from cells for chemical characterization (e.g. proteomic analysis). The chemical composition of the mitochondrial outer membrane is one of the factors defining the mitochondrial isoelectric point (p*I*), which is a property useful for the analysis and characterization of isolated mitochondria. We previously used capillary isoelectric focusing (cIEF) with laser-induced fluorescence detection to determine the experimental p*I* of individual mitochondria after their isolation under depolarizing conditions. This technique revealed that, when kept non-functional, mitochondrial p*I* is heterogeneous as displayed by the observed distributions of p*I*. To model the effect of surface composition on p*I* heterogeneity of these mitochondria, we devised a method to predict mitochondrial p*I*s using simulated surface compositions. The method was initially validated by predicting the p*I*s of known mitochondrial outer membrane proteins and then extended to isolated mitochondria, in which both ionizable amino acids and phospholipids contribute to mitochondrial p*I*. After using a Monte Carlo method to generate a library of over two million possible mitochondrial surface compositions, sufficient compositions to match the frequency of occurrence of experimental mitochondrial p*I*s were randomly selected. This comparison allows for association of a given individual mitochondrial p*I* with thousands of randomly chosen compositions. The method predicts significant changes in the percentages of some amino acids and phospholipids for observed p*I* differences between individual mitochondria, which is an important advancement toward explaining the observed heterogeneity of mitochondrial p*I*.

INTRODUCTION

The p*I* of a synthetic or biological particle refers to those conditions that lead to a net surface charge of zero under which the particle does not experience an electrical force in the presence of an electric field. For biological particles such as mitochondria, the surface charge depends on the ionizable functional groups of the molecules on the surface and their transmembrane potential, which arises from an electrochemical gradient across the membrane established to drive metabolic processes within the cell. [1, 2] Measurement of the p*I* of synthetic nanoparticles[3] or non-functional biological particles[4, 5] such as viruses allows for their analytical separation. Calculation of an analyte's p*I* is useful to optimize separation conditions in electrophoresis and to help identify unknowns in isoelectric focusing, a

*Corresponding Author arriaga@umn.edu.

ASSOCIATED CONTENT

Supporting Information. Description of initial conditions, derivation of complete equation for p*I* calculation, comparison to outer mitochondrial membrane proteins including list of proteins, data from comparison of compositions. This material is available free of charge via the Internet at http://pubs.acs.org.

Notes

The authors declare no competing financial interest.

technique in which analytes are separated based on their p*I*. Prediction of protein p*I* from amino acid sequences is a well-established technique,[6] and the p*I* of particles can be predicted based on their surface properties. This has been done with simple particles (e.g. nanoparticles coated with mixtures of two different proteins),[7] but has not been attempted with more complex biological particles with a heterogeneous surface composition. Isoelectric focusing techniques such as gel electrophoresis with immobilized pH gradients and cIEF are powerful separations methods capable of high resolution and excellent peak capacity.[8] While these techniques are typically used to separate proteins, they are adaptable to biological particles; we introduced the use of cIEF to separate individual non-functional mitochondria by p*I*.[9] We determined that mitochondria from a cultured cell line possess a range of p*I*s, a reflection of the biological heterogeneity of their surface compositions.

Here we report a simulation of the mitochondrial outer membrane to investigate heterogeneity in surface composition and model an experimentally determined p*I* distribution of non-functional mitochondria. Monte Carlo methods are used to generate compositions composed of percentages of phospholipids and amino acids; a p*I* is then calculated for each composition. We used the model to produce a distribution of surface compositions matching an experimentally determined mitochondrial p*I* distribution. This model allowed us to examine differences in possible surface compositions with a given p*I* and to compare compositions with different p*I*s, which are essential to assess variations in individual mitochondrial p*I* measurements and to monitor changes in their surface compositions.

MODEL AND SIMULATIONS

Overview of Model

This model is made up of a library of theoretical mitochondrial surface compositions with p*I* from 4 to 9. Each composition can be thought of as a membrane surface made up of different percentages of seven ionizable amino acids and five phospholipids (see Table 1). These compositions are generated by randomly selecting numbers of each amino acid and phospholipid within constraints defined by a set of initial conditions based on literature and theoretical values. The p*I* of each composition is determined by finding the pH at which the net charge of the composition is zero.

Initial Conditions of Model

The initial conditions of the model are defined by different percentages of amino acids and phospholipids contributing to mitochondrial p*I*. The complete proteome of the outer mitochondrial membrane is unknown, so instead of using the relatively limited set of known outer membrane proteins, we determined initial conditions for the amino acid component of the model by defining an “average protein” using information on all known protein sequences contained in the UniProt Knowledgebase protein database (accessed Dec. 18, 2009).[10] It is anticipated that the potential bias is minimal because the composition of the “average protein” is very similar to that of the average composition of the set of known mitochondrial outer membrane proteins (see Table S-2 in the Supporting Information).

We determined that the “average protein” has 351 amino acids, a molecular weight of 45283 Da, and a ratio of 0.04528 mg protein/nmol protein. Assuming ionizable amino acids that contribute to p*I* are located only in hydrophilic domains of the protein on the inside and outside of the mitochondrial outer membrane, and that the inner and outer domains are of equal size, we calculate that each “average protein” has 53 ionizable amino acids on the outer surface of the membrane.

We have included five phospholipids that contribute to mitochondrial p*I* (see Table 1). Our choices were based on previous experimental determinations of phospholipids in mitochondrial outer membranes.[11–15] Based on these determinations, we calculated a ratio of 52.76 mol phospholipid per mol protein in our model. Combining this ratio with our assumptions about the "average protein," we calculate a ratio of 1.0 mol phospholipid per mol ionizable amino acid for the outer membrane surface. These initial conditions (shown in Table 1) are then used by the simulation to generate a library of compositions. See the Supporting Information for a complete description of how the initial conditions were determined.

Hierarchy of Simulation

In this simulation, two programs work together to generate a library of compositions and a match to experimental data. A flowchart of the general scheme of the simulation is shown in Figure 1. The two programs, one to generate the mitochondrial library and one to match the experimental data (boxes with solid red outlines in the flowchart in Figure 1), were written in Matlab (MathWorks, Natick MA, USA) and are available upon request. Input and output data (boxes with blue dashed outlines or green background in the flowchart in Figure 1) was saved as Microsoft Excel or text files. The first program uses a set of initial conditions (Table 1) to generate a library of approximately 2 million possible compositions using a Monte Carlo approach. Each composition had 10000 relevant molecules including both amino acids and phospholipids. Compositions were randomly generated with restrictions that the numbers of each amino acid and phospholipid must represent a composition within 50% and 20%, respectively, of the initial composition (whole number values of amino acids and phospholipids were used in the simulation then converted to percentages for further analysis; we present all data as percentages). These restrictions were selected to achieve a balance between generating a wider variety of compositions and running the program in a reasonable amount of time (i.e. several hours instead of several days). Less variation in the phospholipid composition was allowed because these molecules are thought to be less variable and have been experimentally determined in the mitochondrial outer membrane,[11–15] while the amino acid composition of the mitochondrial outer membrane is likely more variable as it depends on heterogeneity of the mitochondrial surface proteome. Next, the p*I* of each randomly-generated composition is found using the expression for p*I* derived below.

Expression for p*I*

To find the p*I* of each composition, we derived an expression similar to the expression derived by Rezwan et al. to calculate net charge as a function of pH.[7] This expression is in the general form

$$Z(pH)=\sum n_x a_x(pH) \quad (1)$$

where n_x is the number of each amino acid or phospholipid x in the composition of interest and α_x(pH) represents the respective electrical net charge taking into account pH-dependent dissociation of specific functional group of x. The expression and its derivation including relevant amino acids and phospholipids are shown in the Supporting Information (Equations S-1 through S-6). Equation S-6 is solved numerically by varying the pH between 3 and 11, and accepts a solution if $|Z(\text{pH})| < 0.1$. This value was chosen to achieve a balance between accuracy and computation time, and results in calculation of p*I* values < 0.01 pH units of the "true" p*I* value for a given composition. For example, using the initial composition shown in Table 1, a $|Z(\text{pH})| < 0.1$ corresponds to pH values ranging between 4.78596 and 4.78617, (i.e., 0.00021 pH units). The program may be run as long as necessary to generate a library of sufficient size; to generate a library of ~2 million p*I*s with their corresponding

compositions, the program was run for 1.5 hours on four 3.0 GHz dual-core processors. The library is available upon request.

Comparison to Experimental Data

After the library was generated, a subset of simulated compositions was selected to match an experimentally determined mitochondrial p*I* distribution. This experimental data was obtained by cIEF as previously described from a mitochondrial sample consisting of intact mitochondria isolated by differential centrifugation from cultured rat myoblast cells.[9] To select compositions matching the experimental data, the experimental p*I*s of individual mitochondria were represented as a histogram distribution. The bins of this distribution guided a Monte Carlo-based selection of ~ 2000 compositions from the library so that the p*I* distribution of selected compositions matched the experimental p*I* distribution. In total, about two thousand compositions were selected from the library with the frequency of selections of compositions in each bin corresponding to the experimental data.

RESULTS AND DISCUSSION

Validation of Simulation

To validate the method, we compared collections of simulated compositions of a given p*I* to the amino acid compositions of known mitochondrial outer membrane proteins with the same p*I*. Comparison of the average composition of the collection of simulated compositions with the true composition of the test protein determined the suitability of the method to predict protein compositions.

We selected 73 known mitochondrial outer membrane proteins from *Rattus norvegicus* as the test proteins. See the Supporting Information (Table S-4) for the complete list of proteins and their p*I*s. We calculated a p*I* for each protein using the amino acid sequences and Equation S-6 in the Supporting Information (modified to exclude phospholipids). Then, we modified the program to generate compositions with amino acids only. As the program generated compositions, only those compositions with p*I* within 0.02 pH units from the calculated p*I*s of the mitochondrial outer membrane proteins were kept (we selected this range to approximate the resolving power of a typical cIEF experiment). This approach differs from the approach used for the generation of the mitochondrial library (i.e. instead of generating a set of compositions with a wide range of p*I*s, only compositions with p*I*s matching the proteins were generated). We used the program to generate more than 5,000 and up to 150,000 compositions for each of 69 mitochondrial outer membrane proteins, the remaining four proteins had p*I*s that were too high (p*I* 9.64 and above) for compositions to be generated. We then compared the average percent of each amino acid in the generated compositions to the actual percent of that amino acid in the known protein (for plots of these comparisons, see Figure S-1 in the Supporting Information). As expected, the percentages of the acidic (asp, glu) and basic (lys, arg) amino acids depend more strongly on p*I* than the percentages of the other amino acids. This comparison to known sequences is demonstrated in Figure 2, in which the average difference in percent composition from the known amino acid composition of each sequence is plotted against the p*I* of the known sequence. In these plots, many of the data points fall within one standard deviation of zero, and the majority of compositions differ by less than 10% for each amino acid. Smaller proteins may lack a certain type of amino acid completely or have p*I*s outside the range which the model can produce (since the initial conditions and restrictions of the model dictate a minimum percentage of the acidic and basic amino acids). For instance, the protein connexin 43 (Q6Q6S2, IPI00231746) was identified as an outer mitochondrial membrane protein with calculated p*I* of 9.52. This protein has a sequence of only 29 amino acids, six of which are ionizable amino acids. While the simulation could generate compositions with a p*I* of 9.52,

these compositions were not a good match for the six ionizable amino acids found in connexin 43. Despite limitations with small proteins, the model is overall adequate to predict amino acid compositions of known mitochondrial proteins with ~ 10% precision.

Distribution of amino acids and phospholipids in the library of compositions

The ideal library must include compositions representing the abundance of all ionizable groups at each p*I*. By examining approximately two million randomly generated compositions of the library through scatterplots of the percent of each amino acid or phospholipid versus p*I*, it became apparent that all the generated compositions had p*I*s between 4 and 9, but were not uniformly distributed (Figure 3). Areas which appear darker in the plots contain more data points, representing more individual compositions with similar p*I*s. There were significantly more compositions with p*I* from 4 to 6 than from 6 to 9. This lack of uniformity depends on the initial percentage, pK_a, and restrictions on the allowable range of each amino acid or phospholipid. We arbitrarily restricted the variation in composition of each phospholipid and amino acid to 20% and 50%, respectively, as this reduced the computational time while maintaining compositions that are likely within the expected deviations of the typical compositions dictated by the “average protein” composition. Allowing for more variation would increase the ranges of individual amino acids and phospholipids in the compositions, and slightly increase the range of generated p*I*s, but the general trends would likely remain the same. Predictably, compositions with higher p*I*s tend to have higher percentages of basic amino acids such as lys and arg, and compositions with lower p*I*s tend to have higher percentages of acidic amino acids such as glu and asp. Importantly, the arbitrarily set ranges for phospholipids and amino acids did not exclude less probable compositions (e.g. a composition with p*I* of 9 but a relatively low percentage of one basic amino acid such as lys, these compositions are located in areas of the plots which appear lighter) from the library.

Comparison to an Experimental p*I* Distribution

To model an experimental p*I* distribution, we sampled the library to collect compositions associated with experimental p*I*s. We sampled a relatively small number of compositions (~ 2000 out of 2 million) to mirror a cIEF experiment in which a similar number of individual mitochondria are analyzed. Mitochondrial p*I* distributions, like many experimental results obtained from biological sources, are non-normal distributions and are therefore best evaluated by non-parametric statistical methods which preserve the shape of the distribution. The experimental and predicted mitochondrial p*I* distributions are shown in Figure 4A. The experimental distribution represents 121 individual mitochondria with p*I* from 4.66 to 6.83, and the predicted distribution represents 1998 compositions. The number of bins used to represent the distributions was selected based on the total number of individual mitochondria in the experimental data using a statistics formula which recommends a minimum bin number for representing nonparametric data.[20] While the experimental distribution in Figure 4A appears to be non-normal, we are able to match this distribution by selecting compositions from the library in a bin-by-bin fashion.

A quantile-quantile (Q-Q) plot is a graphical method to compare two non-normal distributions. Percentiles in increments of 5% from the 5th to 95th percentiles of each p*I* distribution were calculated, and then the percentiles from the predicted mitochondrial p*I* distribution were plotted against the percentiles from the experimental mitochondrial p*I* distribution (Figure 4B). Points in a Q-Q plot of identical distributions would all fall on a 45° line drawn from the origin; deviations from the line indicate differences in the distributions. We can also compare these distributions by calculating the sum of squares of the residuals (ss_{res}) of the quantiles in the Q-Q plot. For the Q-Q plot shown in Figure 4B, $ss_{res} = 0.121$. We find that our predicted distribution is as similar to the experimental

distribution as replicate experimental cIEF measurements of the same mitochondrial sample (ss_{res} = 0.150).[9] Therefore, the collection of simulated compositions selected to match the experimental data is an appropriate model for comparison.

Comparison of Compositions with Different p*I*

To demonstrate the utility of our method in describing the differences in sets of compositions for a given p*I*, we selected several p*I*s from different bins of the histogram in Figure 4A to compare. As a starting point, we selected a p*I* from the bin with the highest frequency of compositions (6.77), and compared it to a p*I* with the smallest difference typically resolvable by cIEF (6.75), a p*I* from the adjacent bin (6.41), and a p*I* from a distant bin (4.93). The average and standard deviation of the percentage of each amino acid or phospholipid in all compositions from the library within 0.01 pH units of each p*I* were then calculated (see Supporting Information, Table S-5). The average difference in each amino acid or phospholipid from the composition with p*I* 6.77 is shown in Figure 5 (also see Supporting Information, Table S-6). The largest differences in the compositions are in the acidic and basic amino acids between the compositions with the greatest difference in p*I*. However, significant differences are detected in some amino acids and phospholipids even between the two closest p*I*s (e.g. in glu or his). Since some differences are more pronounced than others, we distinguish between differences which are significant at the 95% confidence level ($p < 0.05$) and differences which are significant with greater than 99.9% confidence ($p < 0.001$). This method of comparison could be modified depending on the goal of the analysis; for instance, it might be useful to combine acidic amino acids such as asp and glu and basic amino acids such as lys and arg when comparing collections of compositions with larger differences in p*I* (i.e. 6.77 compared to 4.93) since these amino acids show similar trends. However, the differences in these amino acids do not follow the same trends when comparing compositions with p*I* values which are closer together (i.e. 6.77 compared to 6.75 or 6.41). This type of analysis could also be used to determine amino acids or phospholipids that have a greater effect on p*I* over larger p*I* ranges (e.g. comparing compositions with p*I* 7.00 ± 1.00 to compositions with p*I* 6.00 ± 1.00). Overall, these results demonstrate the ability of the model to describe differences in composition between collections of individual compositions with different p*I*.

Potential Applications of Model

This model provides a simulation of the mitochondrial outer membrane and the dependence of mitochondrial p*I* on the amino acid and phospholipid composition of the membrane, and allows an experimental p*I* distribution to be modeled. We can envision many potential applications and future refinements for this model. Post-translational modifications, damage to proteins or phospholipids, and changes in the relative amounts of specific proteins or phospholipids in the outer mitochondrial membrane are all biologically relevant processes which could be simulated with this model. The model could also be applied to other synthetic or biological particles.

Post-translational modifications to proteins in the mitochondrial outer membrane could result in a change in p*I* of the protein or mitochondrial composition. For example, phosphorylation of serine or threonine is a common post-translational modification involved in many protein signaling cascades that results in an addition of two negative charges to a protein; this modification would lower the p*I* of a mitochondrion. Future refinements in the model could be made to predict the effects of different extents of phosphorylation at specific sites. The effects of other post-translational modifications important in mitochondrial signaling such as ubiquitination could be predicted. Ubiquitination of outer mitochondrial membrane proteins is an important step in targeting damaged mitochondria for elimination by the cellular process of mitophagy.[21] This process is known to be affected in several

disease states and changes in mitophagy are thought to be associated with aging.[22] Ubiquitination involves the addition of one or more ubiquitin proteins to the side chain of lys, resulting in an increase in the number of ionizable amino acids but a net decrease in p*I* (ubiquitin has a p*I* of 6.56). Different p*I*s associated with ubiquitinylated compositions could be simulated, and this information could be used to design new experiments to analyze mitochondria marked for degradation by mitophagy.

This model could be extended to predict the effects of damage to proteins and phospholipids on mitochondrial p*I*. For instance, protein damage in the form of carbonylation of lys, arg, and his would result in changes to protein p*I*.[23] Protein carbonylation is thought to be caused by increased mitochondrial production of reactive oxygen species, and is associated with cancer, neurodegenerative disease, and other age-related diseases.[24] Our model could be used to produce compositions associated with mitochondrial outer membranes containing different degrees of carbonylated proteins.

This model could be used to predict the effect of over- or under-expression of proteins relative to phospholipids in the outer mitochondrial membrane. For example, we generated a new composition with a 10% reduction in its total protein percentage by reducing each amino acid by 10% of its initial value from the average composition for p*I* 6.77 and keeping the phospholipid percentages constant (see Table S-7 in the Supporting Information). The p*I* of this new composition is 6.30, a relatively large decrease of 0.47. A further extension of this idea is to predict the effect of underexpression of a known protein on the p*I* of a given composition. For example, the protein Fis1, with a p*I* of 8.88, is involved in mitochondrial fission, a process that affects mitochondrial morphology[25] and regulates degradation of damaged mitochondria in the cell.[26] Mitochondria lacking the normal amount of this protein could be excluded from the turnover process and become dysfunctional. Assuming that Fis1 represents 1% of the total mitochondrial outer membrane proteins, we generated a new composition representing a 50% decrease of Fis1 from the average composition for p*I* 6.77 (see Table S-7 in the Supporting Information). This was done by reducing the percentage of each amino acid in the p*I* 6.77 composition by an amount proportional to the amount in which they are found in Fis1 (while keeping the percentages of phospholipids constant). The p*I* of this new composition is 6.73, a decrease of 0.04. While small, this p*I* difference could be resolved by cIEF. Using this approach, shifts in a mitochondrial p*I* distribution due to protein expression changes could be determined and used to design experiments or optimize separation conditions. Likewise, changes in p*I* due to changes in the phospholipid composition of the mitochondrial outer membrane could be predicted with this model. Since mitochondrial phospholipid composition directly affects many mitochondrial processes,[27] changes in phospholipid composition could represent biologically important processes or differences in mitochondrial function. For instance, translocation of oxidized cardiolipin to the outer mitochondrial membrane has been suggested to be involved in apoptosis.[28] The effect on p*I* of the increase in cardiolipin in the outer membrane could be predicted and used to design an experiment to study this process.

This method could also be adapted to other biological or synthetic particles such as cells, other organelles, or nanoparticles by changing the initial conditions involved in the prediction. For instance, identification of microorganisms by cIEF is a promising technique for sensitive and selective characterization of different bacterial strains;[29] our method could be used to predict their surface compositions or to predict changes in their p*I*s upon modifications known to occur to their surface.

Our model could also be the basis to develop models for functional mitochondria that take into account their transmembrane potential, a factor that contributes to charge accumulation at the surface of biological membranes.[1, 2] Experimental conditions conducive to support

functional mitochondria during isoelectric focusing could make it possible to investigate individual mitochondrial membrane potentials by cIEF. This will make it possible to incorporate previous models of the dependence of electrophoretic mobility on membrane potential[30–32] and transmembrane pH gradients[33–35] into predictions of p*I* of individual functional mitochondria. This additional experimental work, combined with future refinements to our model, could shed light on such unknowns as the dependence of mitochondrial p*I* on the surface charge of the mitochondrial inner membrane and the effects of the isoelectric focusing technique itself on mitochondrial membrane potential.

CONCLUSIONS

We use a Monte Carlo method to produce individual compositions of the mitochondrial outer membrane with different percentages of amino acids and phospholipids to model the heterogeneity of mitochondrial p*I*. This method is able to match an experimentally-determined p*I*s distributions of nonfunctional mitochondria and make predictions about the individual compositions associated with experimental p*I*s. We validated the method by predicting the amino acid compositions of known mitochondrial outer membrane proteins. The model can be used to predict changes in p*I* upon changes to surface composition.

Supplementary Material

Refer to Web version on PubMed Central for supplementary material.

Acknowledgments

This work was supported by the National Institutes of Health (Grant R01-AG020866). G.G.W. was supported in part by NIH Training Grant T32-AG029796. B.J.F was supported in part by the North Star STEM Alliance. A.N. was supported in part by a UROP award from the University of Minnesota. This work was carried out in part using computing resources at the University of Minnesota Supercomputing Institute.

REFERENCES

1. Dukhin AS. Biospecific Mechanism of Double-Layer Formation and Peculiarities of Cell Electrophoresis. Colloids Surf. A. 1993; 73:29–48.
2. Dukhin AS, Ulberg ZR, Karamushka VI, Gruzina TG. Peculiarities of live cells' interaction with micro- and nanoparticles. Adv. Colloid Interface Sci. 2010; 159(1):60–71. [PubMed: 20637326]
3. Pyell U. Characterization of nanoparticles by capillary electromigration separation techniques. Electrophoresis. 2010; 31(5):814–831. [PubMed: 20191544]
4. Michen B, Graule T. Isoelectric points of viruses. J. Appl. Microbiol. 2010; 109(2):388–397. [PubMed: 20102425]
5. Subirats X, Blaas D, Kenndler E. Recent developments in capillary and chip electrophoresis of bioparticles: Viruses, organelles, and cells. Electrophoresis. 2011; 32(13):1579–1590. [PubMed: 21647924]
6. Bjellqvist B, Hughes GJ, Pasquali C, Paquet N, Ravier F, Sanchez JC, Frutiger S, Hochstrasser D. The focusing positions of polypeptides in immobilized pH gradients can be predicted from their amino acid sequences. Electrophoresis. 1993; 14(10):1023–1031. [PubMed: 8125050]
7. Rezwan K, Meier LP, Gauckler LJ. A prediction method for the isoelectric point of binary protein mixtures of bovine serum albumin and lysozyme adsorbed on colloidal titania and alumina particles. Langmuir. 2005; 21(8):3493–3497. [PubMed: 15807593]
8. Shimura K. Recent advances in IEF in capillary tubes and microchips. Electrophoresis. 2009; 30(1): 11–28. [PubMed: 19107704]
9. Wolken GG, Kostal V, Arriaga EA. Capillary isoelectric focusing of individual mitochondria. Anal. Chem. 2011; 83(2):612–618. [PubMed: 21192658]

10. The-Uniprot-Consortium, Reorganizing the protein space at the Universal Protein Resource (UniProt). Nucleic Acids Res. 2012; 40(D1):D71–D75. [PubMed: 22102590]
11. Hovius R, Lambrechts H, Nicolay K, Dekruijff B. Improved methods to isolate and subfractionate rat-liver mitochondria. Lipid composition of the inner and outer membrane. Biochim. Biophys. Acta. 1990; 1021(2):217–226. [PubMed: 2154259]
12. deKroon A, Dolis D, Mayer A, Lill R, deKruijff B. Phospholipid composition of highly purified mitochondrial outer membranes of rat liver and Neurospora crassa. Is cardiolipin present in the mitochondrial outer membrane? Biochim. Biophys. Acta, Biomembr. 1997; 1325(1):108–116.
13. Hovius R, Thijssen J, Vanderlinden P, Nicolay K, Dekruijff B. Phospholipid asymmetry of the outer membrane of rat liver mitochondria: Evidence for the presence of cardiolipin on the outside of the outer membrane. FEBS Lett. 1993; 330(1):71–76. [PubMed: 8370463]
14. Liu JH, Dai Q, Chen J, Durrant D, Freeman A, Liu T, Grossman D, Lee RM. Phospholipid scramblase 3 controls mitochondrial structure, function, and apoptotic response. Mol. Cancer Res. 2003; 1(12):892–902. [PubMed: 14573790]
15. Gebert N, Joshi AS, Kutik S, Becker T, McKenzie M, Guan XL, Mooga VP, Stroud DA, Kulkarni G, Wenk MR, Rehling P, Meisinger C, Ryan MT, Wiedemann N, Greenberg ML, Pfanner N. Mitochondrial cardiolipin involved in outer-membrane protein biogenesis: implications for Barth syndrome. Curr. Biol. 2009; 19(24):2133–2139. [PubMed: 19962311]
16. Bjellqvist B, Basse B, Olsen E, Celis JE. Reference points for comparisons of 2- dimensional maps of proteins from different human cell types defined in a pH scale where isoelectric points correlate with polypeptide compositions. Electrophoresis. 1994; 15(3–4):529–539. [PubMed: 8055880]
17. Moncelli MR, Becucci L, Guidelli R. The intrinsic pK_a values for phosphatidylcholine, phosphatidylethanolamine, and phosphatidylserine in monolayers deposited on mercury electrodes. Biophys. J. 1994; 66(6):1969–1980. [PubMed: 8075331]
18. Tsui FC, Ojcius DM, Hubbell WL. The intrinsic pK_a values for phosphatidylserine and phosphatidylethanolamine in phosphatidylcholine host bilayers. Biophys. J. 1986; 49(2):459–468. [PubMed: 3955180]
19. Kates M, Syz JY, Gosser D, Haines TH. pH-dissociation characteristics of cardiolipin and its 2'-deoxy analogue. Lipids. 1993; 28(10):877–882. [PubMed: 8246687]
20. Terrell GR, Scott DW. Oversmoothed Nonparametric Density Estimates. J. Am. Stat. Assoc. 1985; 80(389):209–214.
21. Narendra DP, Youle RJ. Targeting mitochondrial dysfunction: role for PINK1 and Parkin in mitochondrial quality control. Antioxid. Redox Signal. 2011; 14(10):1929–1938. [PubMed: 21194381]
22. Green DR, Galluzzi L, Kroemer G. Mitochondria and the Autophagy-Inflammation-Cell Death Axis in Organismal Aging. Science. 2011; 333(6046):1109–1112. [PubMed: 21868666]
23. Amici A, Levine RL, Tsai L, Stadtman ER. Conversion of amino acid residues in proteins and amino acid homopolymers to carbonyl derivatives by metal-catalyzed oxidation reactions. J. Biol. Chem. 1989; 264(6):3341–3346. [PubMed: 2563380]
24. Nystrom T. Role of oxidative carbonylation in protein quality control and senescence. EMBO J. 2005; 24(7):1311–1317. [PubMed: 15775985]
25. Stojanovski D, Koutsopoulos OS, Okamoto K, Ryan MT. Levels of human Fis1 at the mitochondrial outer membrane regulate mitochondrial morphology. J. Cell. Sci. 2004; 117(7): 1201–1210. [PubMed: 14996942]
26. Twig G, Elorza A, Molina AJA, Mohamed H, Wikstrom JD, Walzer G, Stiles L, Haigh SE, Katz S, Las G, Alroy J, Wu M, Py BF, Yuan J, Deeney JT, Corkey BE, Shirihai OS. Fission and selective fusion govern mitochondrial segregation and elimination by autophagy. EMBO J. 2008; 27(2): 433–446. [PubMed: 18200046]
27. Osman C, Voelker DR, Langer T. Making heads or tails of phospholipids in mitochondria. J. Cell. Biol. 2011; 192(1):7–16. [PubMed: 21220505]
28. Korytowski W, Basova LV, Pilat A, Kernstock RM, Girotti AW. Permeabilization of the mitochondrial outer membrane by Bax/truncated Bid (tBid) proteins as sensitized by cardiolipin hydroperoxide translocation. Mechanistic implications for the intrinsic pathway of oxidative apoptosis. J. Biol. Chem. 2011; 286(30):26334–26343. [PubMed: 21642428]

29. Horka M, Horky J, Kubesova A, Zapletalova E, Slais K. The trace analysis of microorganisms in real samples by combination of a filtration microcartridge and capillary isoelectric focusing. Anal. Bioanal. Chem. 2011; 400(9):3133–3140. [PubMed: 21499678]

30. Kamo N, Muratsugu M, Kurihara K, Kobatake Y. Change in Surface-Charge Density and Membrane-Potential of Intact Mitochondria during Energization. FEBS Lett. 1976; 72(2):247–250. [PubMed: 16386033]

31. Aiuchi T, Kamo N, Kurihara K, Kobatake Y. Significance of surface-potential in interaction of 8-anilino-1-naphthalenesulfonate with mitochondria - fluorescence intensity and zeta potential. Biochemistry. 1977; 16(8):1626–1630. [PubMed: 856252]

32. Tsoneva IC, Tomov TC. Relationship between the Power of Energization and the Electrophoretic Mobility of Rat-Liver Mitochondria. Bioelectroch. Bioener. 1984; 12(3–4):253–258.

33. Phayre AN, Farfano HMV, Hayes MA. Effects of pH gradients on liposomal charge states examined by capillary electrophoresis. Langmuir. 2002; 18(17):6499–6503.

34. Chen Y, Arriaga EA. Individual electrophoretic mobilities of liposomes and acidic organelles displaying pH gradients across their membranes. Langmuir. 2007; 23(10):5584–5590. [PubMed: 17402758]

35. Pysher MD, Hayes MA. Examination of the electrophoretic behavior of liposomes. Langmuir. 2004; 20(11):4369–4375. [PubMed: 15969140]

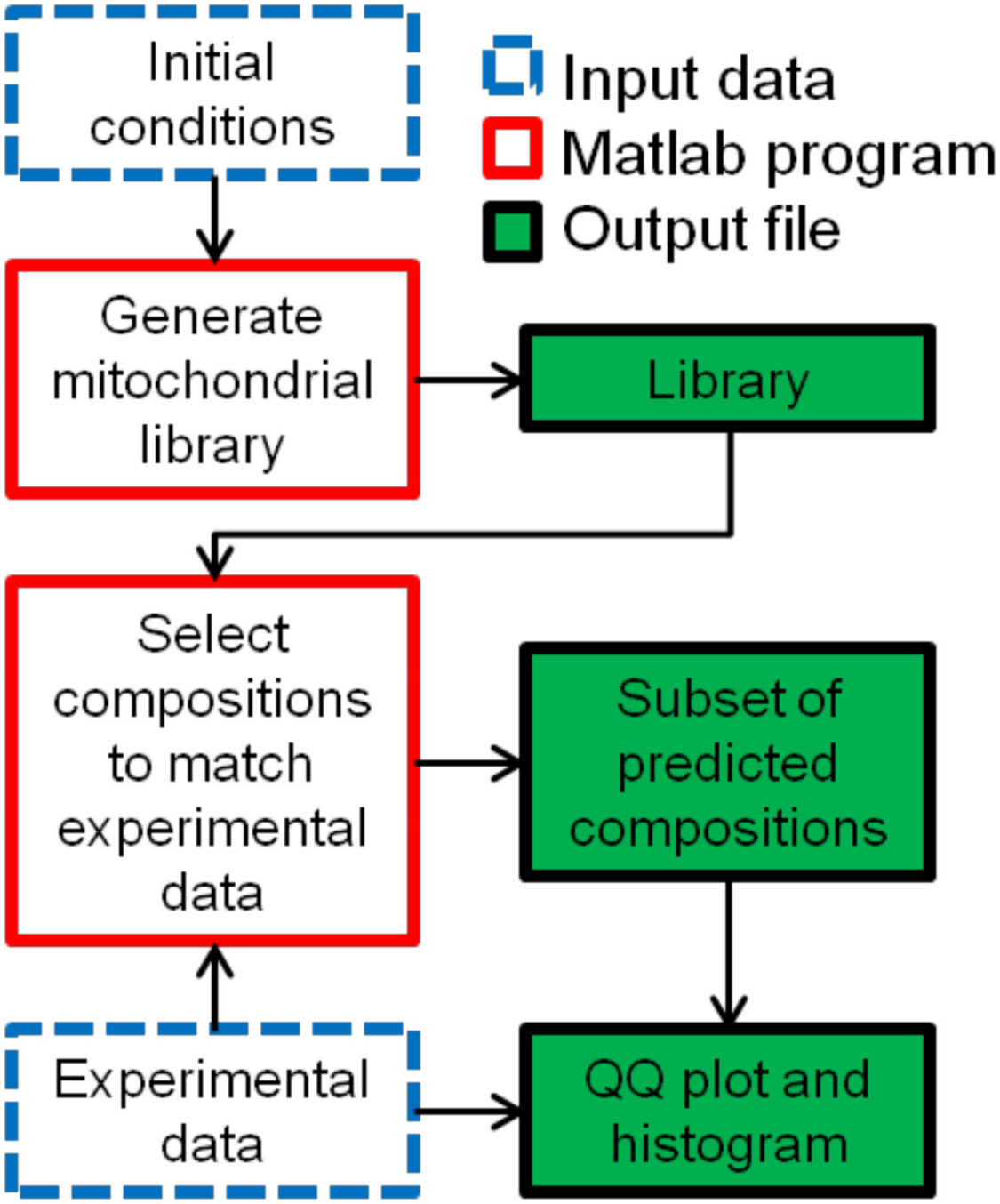

Figure 1.
Flowchart of programs to generate mitochondrial library and match experimental data.

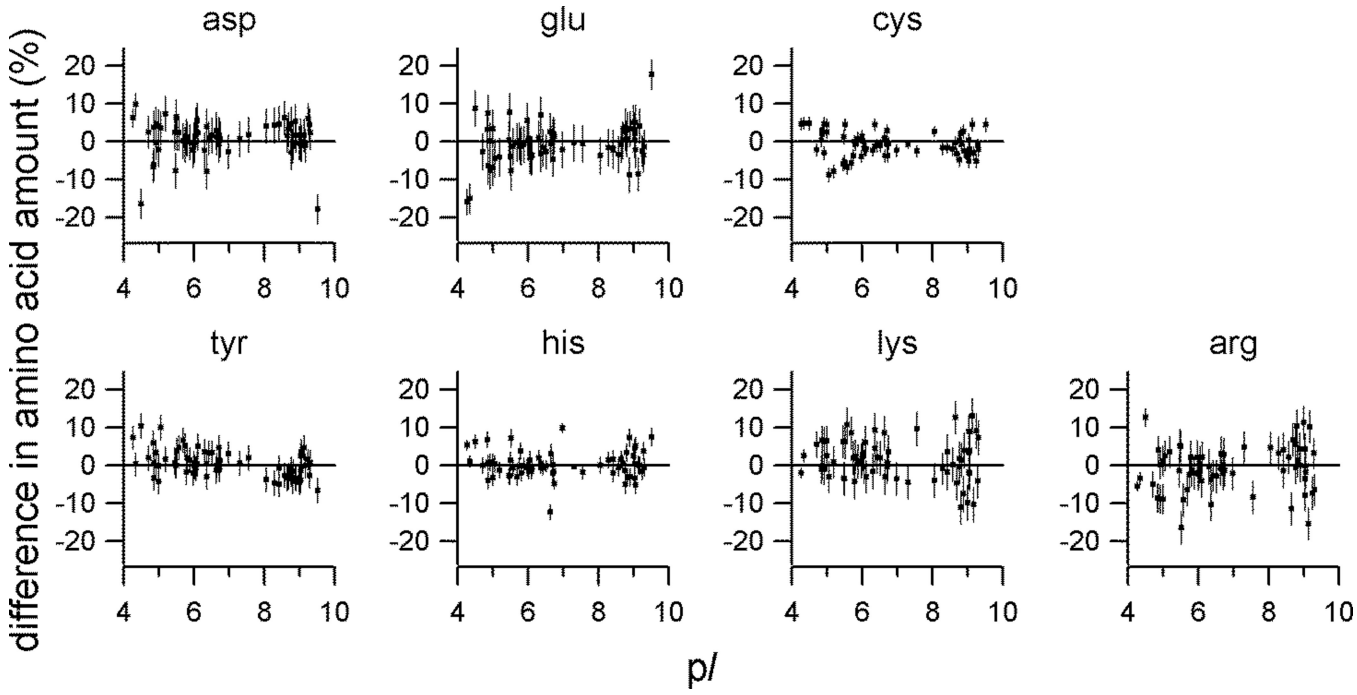

Figure 2.

Comparison of predicted compositions to known compositions of mitochondrial outer membrane proteins. Deviation in average amino acid percentage in the predicted compositions (with similar p*I* of ± 0.02) from the actual composition of known mitochondrial outer membrane proteins plotted against p*I*. Error bars are plus/minus one standard deviation of the average difference from the known composition.

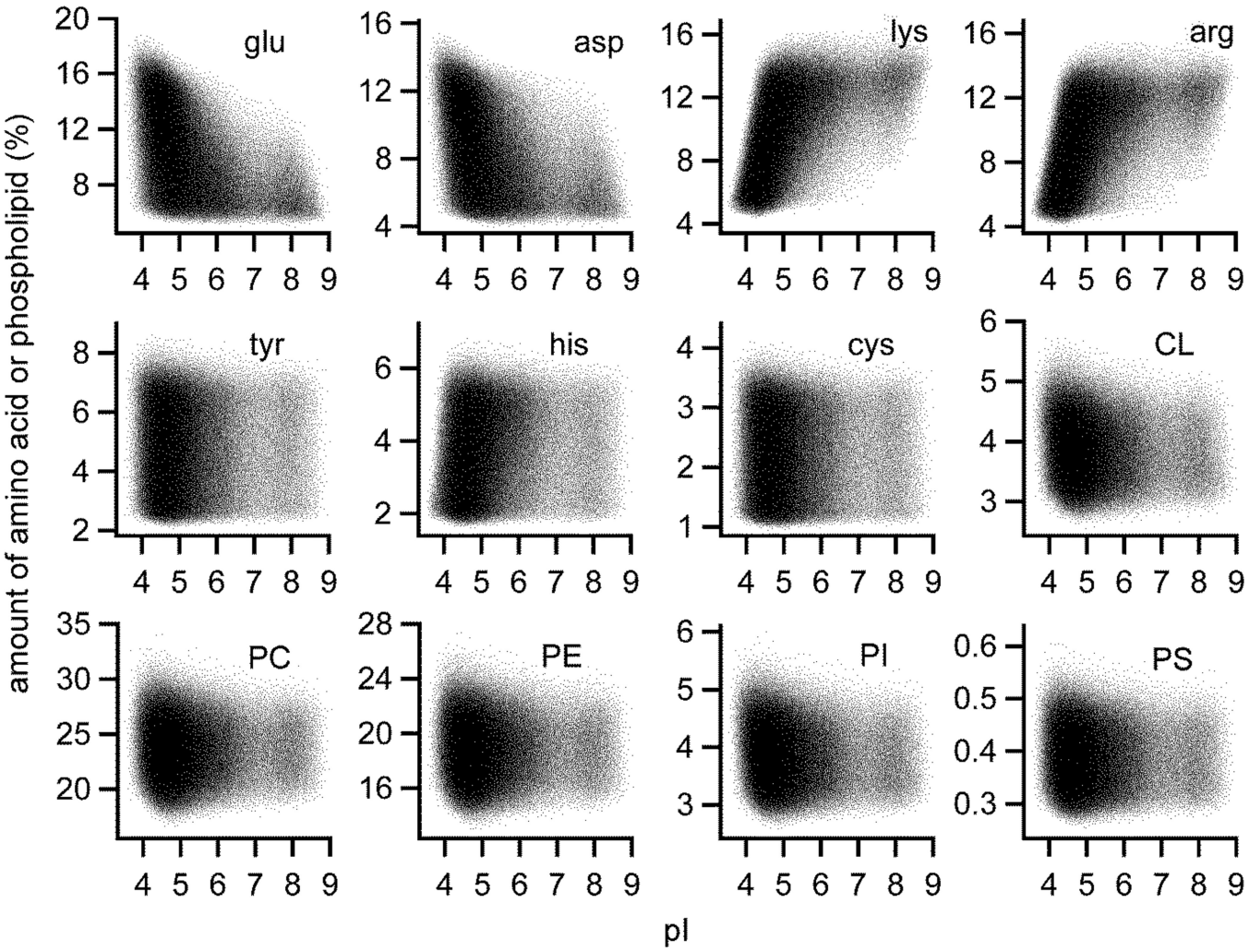

Figure 3.
Trends in percentages of each amino acid or phospholipid vs. p*I* for all compositions in the library.

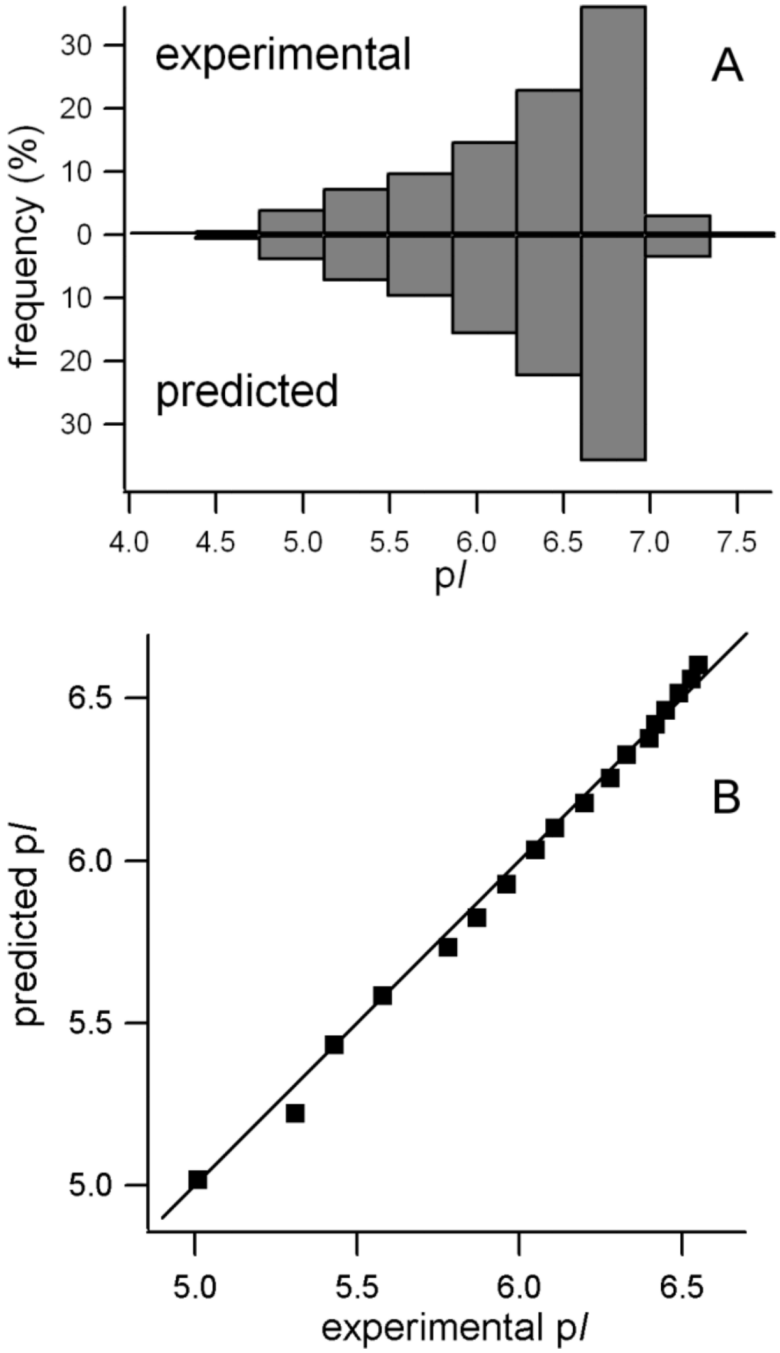

Figure 4.
(A) Experimental and predicted mitochondrial isoelectric point distributions. (B) Q-Q plot comparison of predicted to experimental mitochondrial p*I* distributions.

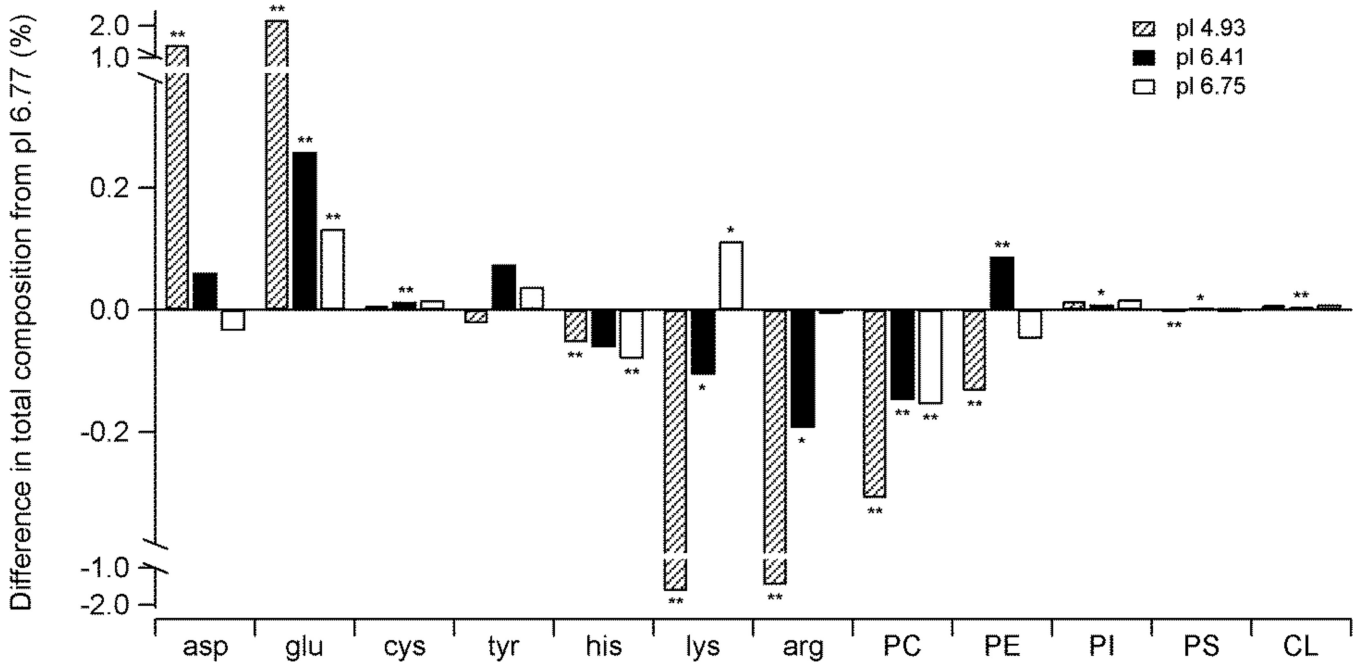

Figure 5.

Comparison of compositions with p*I* 6.77 ± 0.01 to compositions with other p*I*s. Statistical significance was determined using t-tests (two-tailed, equal variance), * indicates $p < 0.05$; ** indicates $p < 0.001$.

Table 1

Initial conditions.

Amino acids and phospholipids	Ionizable functional group(s)	pK_a	Initial composition (mol %)
aspartic acid (asp)	carboxy	4.05	9.06
glutamic acid (glu)	carboxy	4.45	11.26
cysteine (cys)	sulfhydryl	9.00	2.26
tyrosine (tyr)	phenol	10.00	4.84
histidine (his)	imidazole	5.98	3.78
lysine (lys)	amine	10.00	9.75
arginine (arg)	guanidino	12.00	9.21
phosphatidylcholine (PC)	phosphate, quaternary ammonium cation	0.8, n/a	23.72
phosphatidylethanolamine (PE)	phosphate, amine	0.5, 9.6	18.91
phosphatidylinositol (PI)	phosphate	1.0	2.94
phosphatidylserine (PS)	phosphate, carboxy, amine	2.3, 3.6, 9.8	0.39
cardiolipin (CL)	phosphate, phosphate	2.8, 8.5	3.89
Total			**100%**

pK_as for amino acids were taken according to Bjellqvist et al. [16] pK_{a1} for PC, PE, and PS was determined by Moncelli et al. [17] pK_{a2} for PE and pK_{a2}, pK_{a3} for PS were determined by Tsui et al. [18] pK_as for CL were determined by Kates et al. (the authors determined pK_{a2} for CL to be between 7.5 and 9.5, we use an estimate of 8.5). [19] The pK_a for PI was estimated to be 1.0 based on the pK_as of the other phosphate groups.